

Thermal conductivity of multiphase particulate composite materials

M. Porfiri · N. Q. Nguyen · N. Gupta

Received: 20 November 2007 / Accepted: 7 October 2008 / Published online: 6 November 2008
© Springer Science+Business Media, LLC 2008

Abstract Hollow particle filled composites, called syntactic foams, are used in weight sensitive structural applications in this paper. In this paper, homogenization techniques are used to derive estimates for thermal conductivity of hollow particle filled composites. The microstructure is modeled as a three-phase system consisting of an air void, a shell surrounding the air void, and a matrix material. The model is applicable to composites containing coated solid particles in a matrix material and can be further expanded to include additional coating layers. The model is successful in predicting thermal conductivity of composites containing up to 52% particles by volume. Theoretical results for thermal conductivity are validated with the results obtained from finite element analysis and are found to be in close agreement with them. A simplified approximation of the theoretical model applicable to thin shells is also validated and found to be in good agreement with the corresponding finite element results. The model is applicable to a wide variety of particulate composite materials and will help in tailoring the properties of particulate composites as per the requirements of the application.

Introduction

Enhancement in the understanding of porous materials, such as foams, has resulted in their increased applications in ship, aircraft, and spacecraft structures. A special class of porous materials, called syntactic foams, is synthesized by embedding hollow particles in matrix materials [1, 2]. The presence of porosity inside thin stiff shells of hollow particles results in higher specific stiffness and strength of these composites compared to open-cell and closed-cell foams containing gas porosity in the matrix material. Therefore, syntactic foams are considered very promising lightweight materials in load bearing applications. The hollow particles, called microballoons, are generally made of glass [3], carbon [4], or polymers [5]. Various types of polymeric and metallic materials are widely used as matrices [6–8]. Syntactic foams have been extensively studied for mechanical properties and fracture characteristics under compressive [8–10], tensile [11–14], dynamic [15], and flexural [16, 17] loading conditions.

The use of syntactic foams in thermal insulation is increasing in recent years since incorporation of air filled hollow ceramic particles in polymeric or metallic matrix results in lower thermal conductivity and higher dimensional stability [18, 19]. Some of the pipes used in recovering oil from ultra-deep oil wells have a structure of two concentric pipes with syntactic foam filled in between for thermal insulation and sealing. High temperature variants of syntactic foams have potential to be used in the spacecraft thermal protection systems. These applications require understanding of thermal conductivity in addition to mechanical properties. While studies on mechanical properties of syntactic foams are readily available, studies on thermal properties of these materials are relatively scarce [18]. Considering the recent and potential high temperature applications of syntactic

M. Porfiri · N. Q. Nguyen · N. Gupta (✉)
Department of Mechanical and Aerospace Engineering,
Polytechnic Institute of New York University,
Brooklyn, NY 11201, USA
e-mail: ngupta@poly.edu

M. Porfiri
e-mail: mporfiri@poly.edu

N. Q. Nguyen
e-mail: nnguye02@students.poly.edu

foams, it is required that thermal properties of these materials are characterized. Rigorous mathematical models that can correlate the thermal conductivity of syntactic foams with the properties and volume fractions of the constituent materials are required.

One of the most frequently used methods to derive effective thermal properties of particulate composites is the Rayleigh's method [20]. This method has been used to find thermal properties of two-phase composites where spherical particles are dispersed in simple cubic [21], body centered cubic, and face centered cubic [22] lattice arrangements in a matrix resin. This method can incorporate the particle-matrix interfacial conditions and has been used to study the effects of imperfect interfaces on the effective conductivity of two-phase composites [23]. The method has also been used to analyze the effective thermal conductivity of three-phase composite materials comprising periodic arrays of coated cylinders [24] and coated spheres [25].

As an alternative to Rayleigh's method, homogenization techniques can be used to characterize the effective thermal properties of composite materials. These techniques have been applied to the estimation of effective elastic constants of composite materials [26–28]. Homogenization techniques are considered to be more theoretically grounded than Rayleigh's method and more versatile in the analysis of complicated microstructures. Using homogenization techniques the determination of the effective properties reduces to the solution of a representative thermal problem defined on a unit cell that characterizes the composite's microstructure.

Both the homogenization technique and the Rayleigh's method assume a periodic structure for the particulate composite. Even if particulate composites are generally not periodic, results from these method can be used to build differential schemes similar to those presented in [29, 30] for analyzing mechanical properties of solid particles filled composites with random microstructures and high volume fraction of particles. Unlike empirical models as those summarized in [18, 31], the homogenization technique provides a mathematical exact expression for the thermal conductivity of particulate composites whose inclusions are periodically arranged in the matrix material.

The present research is focused on developing an analytical model to determine the thermal conductivity of syntactic foams using homogenization techniques. Syntactic foams are modeled as a three-phase microstructure where microballoons are regarded as an inner sphere (air) enclosed by a glass shell, which is embedded in a matrix material. Hence, the model is expected to be applicable for a wide variety of particulate composites apart from syntactic foams, especially those containing solid particles coated with a second phase and then embedded in a matrix material. The proposed model builds on the mathematical

tools developed in [32] for analyzing solid particles filled composites. The theoretical findings are extensively validated with finite element analysis (FEA) results obtained by solving a tractable unit cell problem that stems from a thorough analysis of the system's governing equations. The commercial FEA program Ansys is used for the analysis. Several published studies have used FEA methods to determine the thermal conductivity of hollow particles [33] and particulate composites [34, 35].

Problem statement

A typical representative microstructure of syntactic foams is shown in Fig. 1a, where glass microballoons can be seen dispersed in vinyl ester resin matrix. One of the broken microballoons is shown in Fig. 1b, that illustrates

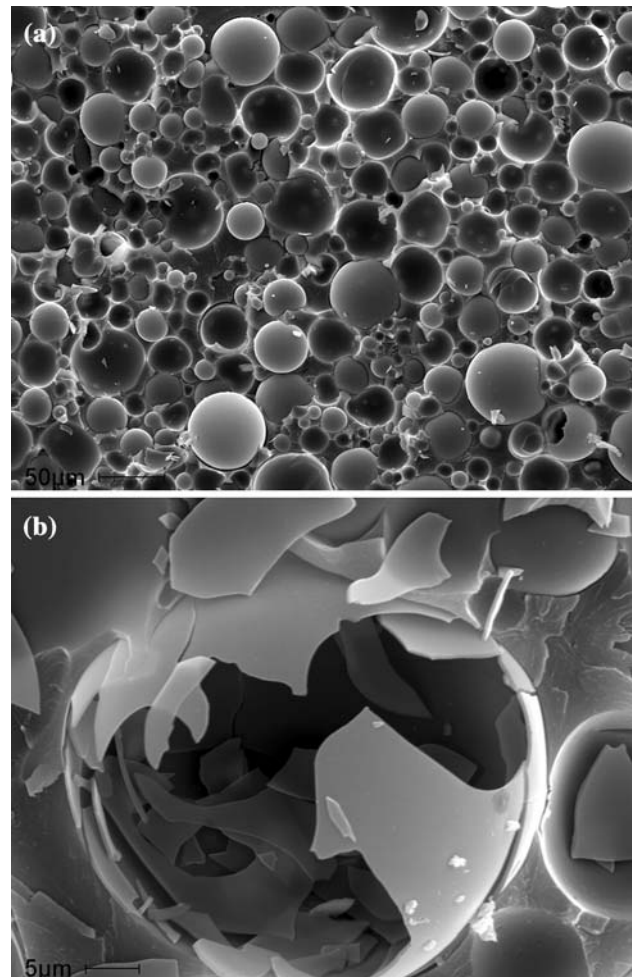


Fig. 1 **a** Microstructure of a syntactic foam containing 60 vol% of glass microballoons in a vinyl ester resin matrix and **b** a broken microballoon showing an air void enclosed within the thin shell

the presence of a large air void inside a thin shell of glass. Typically, microballoons of diameter 10–200 μm and wall thickness of 0.5–2 μm are used in syntactic foams.

Consistent with the microstructure shown in Fig. 1b, the effective thermal conductivity of particulate composites, comprised of an array of identical spheres embedded in a matrix material, is studied. It is assumed that the materials constituting the spherical inclusions, and the matrix are homogenous and isotropic. It is further assumed that the inclusions are dispersed in the matrix in a periodic simple cubic arrangement.

The geometry of the problem, in dimensionless coordinates, is reported in Fig. 2. The distance between the centers of adjacent inclusions is D . The outer radius and shell thickness of inclusions are aD and tD , respectively. The parameters a and t are dimensionless quantities that measure the interdistance between adjacent particles and their shell thickness, respectively. The thermal conductivity of the matrix, of the shell, and of the core are k_m , k_s , and k_c , respectively. Relative conductivities of the shell and of the core are defined as $\tilde{k}_s = k_s/k_m$ and $\tilde{k}_c = k_c/k_m$, respectively. The notations and analytical framework used in what follows are consistent with those used in [32] for solid particle filled composites.

Here and henceforth, \mathcal{E} is the three-dimensional Euclidean point ambient space, e_1, e_2 , and e_3 are orthogonal unit vectors, \mathfrak{o} is a fixed origin in \mathcal{E} , (y_1, y_2, y_3) define a cartesian coordinate system and $y = y_1e_1 + y_2e_2 + y_3e_3$, and (ρ, θ, ϕ) define a spherical coordinate system. $|y|$ refers to the Euclidean norm of y , that is, $|y| = \sqrt{y_1^2 + y_2^2 + y_3^2}$. $Y = (-1/2, 1/2)^3$ denotes the representative unit cell. The domain Ω_r is the sphere of radius r centered at the origin \mathfrak{o} .

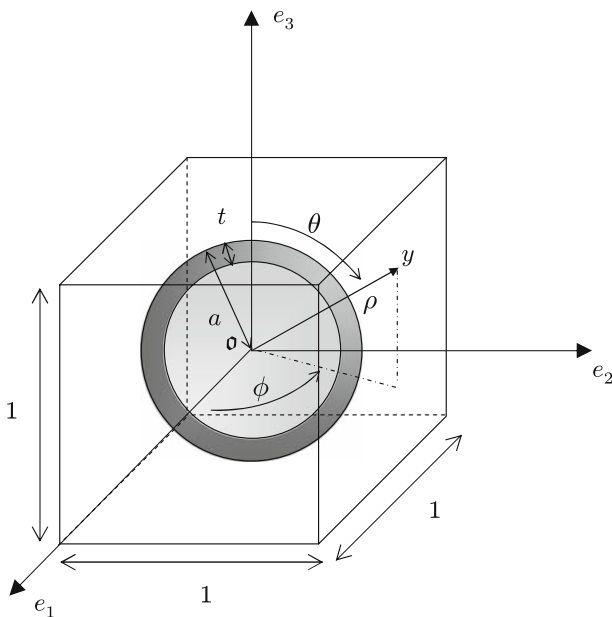


Fig. 2 Geometry of the unit cell problem

The volume of the sphere Ω_r is called f_r , and $f_r = 4 \pi r^3/3$. The domain $\Omega_{r_2,r_1} = \Omega_{r_2} \setminus \Omega_{r_1}$ is the hollow sphere of outer radius r_2 and inner radius r_1 centered at the origin.

The outward unit normal to a regular surface S at y is called $n(y)$. For the spherical surface $\partial\Omega_r$, $v(y)$ is the outward unit normal, that is, $v = y/r$ with $y \in \Omega_r$.

Governing equations

The unit cell problem consists in finding weak solutions $\chi_j \in H^1_{\#}(Y)$, $j = 1, 2, 3$ such that

$$\int_Y \tilde{k}(y) \nabla \varphi(y) \cdot (e_j + \nabla \chi_j(y)) \, dV = 0 \tag{1}$$

for every $\varphi \in H^1_{\#}(Y)$, where $\tilde{k}(y)$ is the relative conductivity with respect to the matrix material, see for example [28]. That is, $\tilde{k}(y) = 1$ if $y \in Y \setminus \Omega_a$, $\tilde{k}(y) = \tilde{k}_s$ if $y \in \Omega_{a,a-t}$, and $\tilde{k}(y) = \tilde{k}_c$ if $y \in \Omega_{a-t}$. Note that χ_j is uniquely determined up to a constant. Due to the symmetries of the problem, it is sufficient to solve (1) for one value of the index j . Here, $j = 3$ is selected and $\chi_3 = \psi$ is set.

A strong formulation of the problem can be derived from (1) through multiple integration by parts

$$\Delta \psi = 0 \quad y \in Y \setminus (\partial\Omega_a \cup \partial\Omega_{a-t}) \tag{2a}$$

$$\psi(y^+) = \psi(y^-) \quad y \in \partial\Omega_a \tag{2b}$$

$$\psi(y^+) = \psi(y^-) \quad y \in \partial\Omega_{a-t} \tag{2c}$$

$$\tilde{k}_s(v \cdot e_3 + v \cdot \nabla \psi(y^+)) = \tilde{k}_c(v \cdot e_3 + v \cdot \nabla \psi(y^-)) \quad y \in \partial\Omega_{a-t} \tag{2d}$$

$$v \cdot e_3 + v \cdot \nabla \psi(y^+) = \tilde{k}_s(v \cdot e_3 + v \cdot \nabla \psi(y^-)) \quad y \in \partial\Omega_a \tag{2e}$$

$$\psi(y) = \psi(y + e_i) \quad i = 1, 2, 3 \quad y \in \partial Y \tag{2f}$$

Effective conductivity

Once the solution of the unit cell problem in Eq. 1 is determined, the relative effective conductivity is found through [28]

$$\tilde{k}^h = \langle \tilde{k}(y) \rangle + \left\langle \tilde{k}(y) \frac{\partial \psi(y)}{\partial y_3} \right\rangle \tag{3}$$

where the spatial average of a Y -periodic function F is defined as

$$\langle F(y) \rangle = \int_Y F(y) \, dV \tag{4}$$

By using Green’s theorem, the second summand in (3) can be transformed into a more manageable summation of surface integrals

$$\begin{aligned} \left\langle \tilde{k}(y) \frac{\partial \psi(y)}{\partial y_3} \right\rangle &= \int_{Y \setminus \Omega_a} \frac{\partial \psi(y)}{\partial y_3} dV + \tilde{k}_s \int_{\Omega_{a-t}} \frac{\partial \psi(y)}{\partial y_3} dV \\ &\quad + \tilde{k}_c \int_{\Omega_{a-t}} \frac{\partial \psi(y)}{\partial y_3} dV \\ &= \int_{\partial Y} \psi(y) n(y) \cdot e_3 dA \\ &\quad + (\tilde{k}_s - 1) \int_{\partial \Omega_a} \psi(y) v(y) \cdot e_3 dA \\ &\quad + (\tilde{k}_c - \tilde{k}_s) \int_{\partial \Omega_{a-t}} \psi(y) v(y) \cdot e_3 dA \end{aligned} \tag{5}$$

Due to the Y -periodicity of the solution, the first summand in the right hand side of (5) vanishes, and the effective relative conductivity (3) can be expressed as

$$\begin{aligned} \tilde{k}^h &= (1 - f_a) + \tilde{k}_s(f_a - f_{a-t}) + \tilde{k}_c f_{a-t} \\ &\quad + (\tilde{k}_s - 1) \int_{\partial \Omega_a} \psi(y) v(y) \cdot e_3 dA \\ &\quad + (\tilde{k}_c - \tilde{k}_s) \int_{\partial \Omega_{a-t}} \psi(y) v(y) \cdot e_3 dA \end{aligned} \tag{6}$$

Rigorous bounds

The effective relative thermal conductivity of the considered particulate composite can be bounded using the two-point bound derived by Hashin and Shtrikman, see for example [28]. The bounds take into consideration only the volume fractions of the different constituents and read

$$\begin{aligned} \left(\frac{f_{a-t}}{2\tilde{k}_{\min} + \tilde{k}_c} + \frac{f_a - f_{a-t}}{2\tilde{k}_{\min} + \tilde{k}_s} + \frac{1 - f_a}{2\tilde{k}_{\min} + 1} \right)^{-1} - 2\tilde{k}_{\min} &\leq \tilde{k}^h \\ \leq \left(\frac{f_{a-t}}{2\tilde{k}_{\max} + \tilde{k}_c} + \frac{f_a - f_{a-t}}{2\tilde{k}_{\max} + \tilde{k}_s} + \frac{1 - f_a}{2\tilde{k}_{\max} + 1} \right)^{-1} - 2\tilde{k}_{\max} \end{aligned} \tag{7}$$

where $\tilde{k}_{\max} = \max\{1, \tilde{k}_c, \tilde{k}_s\}$ and $\tilde{k}_{\min} = \min\{1, \tilde{k}_c, \tilde{k}_s\}$. The theoretically calculated thermal conductivity values will be compared with these bounds for conformity.

Solution of the unit-cell problem

A closed-form solution of the unit cell problem is determined by building on the analytical solution determined in [32] for the case of solid spheres. The solution $\psi(y)$ is expressed as a series expansion of solutions of the Laplace equation. The series coefficients are determined by imposing conditions (2c), (2d), and (2e).

Series solution

The regular solutions to the Laplace equation in spherical coordinates are called v_n , while the solutions that are

singular at the origin are called u_n . The expressions of u_n and v_n are given in the appendix as Eqs. 39a and 39b, respectively. Here, n is used as a multi-index and set as $n = (\sigma, l, m)$, where σ takes values in the set $\{e, o\}$, $l \in \mathbb{Z}^+$, and $m = 0, \dots, l, l - 1$. The set of all admissible multi-indices n is called \mathcal{I} . Further, a subset of indices is defined as $I = \{n \in \mathcal{I} : \sigma = e, l \text{ is even, and } m \text{ is odd}\}$.

Due to the symmetry of the problem, the solution ψ is even in y_1 and y_2 , while it is odd in y_3 . Thus, solutions of the following form are sought

$$\begin{aligned} \psi(y) &= \sum_{n \in I} a_n \sum_{i \in \mathbb{Z}^3} (u_n(y + t_i) - \phi_i(y) \delta_{n,e01}) - f_a a_{e01} v_{e01}(y) \\ y &\in Y \setminus \Omega_a \end{aligned} \tag{8a}$$

$$\psi(y) = \sum_{n \in I} (b_n v_n(y) + c_n u_n(y)) \quad y \in \Omega_{a-t} \tag{8b}$$

$$\psi(y) = \sum_{n \in I} d_n v_n(y) \quad y \in \Omega_{a-t} \tag{8c}$$

where $t_i = i_1 e_1 + i_2 e_2 + i_3 e_3$ with $(i_1, i_2, i_3) \in \mathbb{Z}^3$ and $\phi_i(y) = (1 - \delta_{i,(000)})(u_{e01}(t_i) + y \cdot \nabla u_{e01}(t_i))$ (9)

It is noted that both the summation over the lattice structure in (8a) and the term $-f_a a_{e01} v_{e01}(y) \propto y_3$ are needed for imposing the periodicity condition (2f), see [32]. In addition, the ad-hoc summation for the term $e01$ is needed for assuring the absolute convergence of the infinite summation on i for every $y \in Y$. Indeed, $u_{e01} = O(|i|)$ and the extra term $\phi_i(y)$ guarantees that all the summands in the infinite summation with respect to i have at least the decay rate $|i|^{-4}$. Since the infinite summation on i in (8a) is absolutely convergent, its sum may be computed by squares [36]. Therefore, by accounting for the properties of u_{e01} , see [32], it is found that

$$\psi(y) = \sum_{n \in I} a_n \lim_{R \rightarrow \infty} \sum_{\substack{i \in \mathbb{Z}^3 \\ |t_i| \leq R}} u_n(y + t_i) - f_a a_{e01} v_{e01}(y) \tag{10}$$

In addition, by using the translation properties of u_n , see [32], Eq. 10 can be further simplified into

$$\psi(y) = \sum_{n \in I} a_n \sum_{n' \in \mathcal{I}} (\delta_{n,n'} u_{n'}(y) + S_{nn'} v_{n'}) - f_a a_{e01} v_{e01}(y) \tag{11}$$

where the quantity $S_{n'n}$ is defined by

$$S_{nn'} = \lim_{R \rightarrow \infty} \sum_{\substack{(0,0,0) \neq i \in \mathbb{Z}^3 \\ |t_i| \leq R}} P_{nn'}(y + t_i) \tag{12}$$

and $P_{nn'}$ is the so-called translation matrix for singular solutions of the Laplace equation [32].

Once the coefficients a_n , b_n , c_n , and d_n in (8) are determined, the effective relative thermal conductivity is

obtained through Eq. 6. In particular, by substituting Eq. 8b into 6, by applying Green’s theorem, by using Eqs. 42a and 42b, and by noting that $v(y) \cdot e_3 = \cos\theta = \sqrt{4\pi/3}Y_{e01}$, it can be found that

$$\tilde{k}^h = (1 - f_a) + \tilde{k}_s(f_a - f_{a-t}) + \tilde{k}_c f_{a-t} + \frac{1}{a} \sqrt{\frac{3}{4\pi}} (b_{e01}(f_a(\tilde{k}_s - 1) + f_{a-t}(\tilde{k}_c - \tilde{k}_s)) + c_{e01}f_a(\tilde{k}_c - 1)) \tag{13}$$

Determination of the series coefficients

In order to determine the numerical values of the coefficients $a_n, b_n, c_n,$ and d_n for $n \in I$ appearing in (8), the interface and boundary conditions (2b), (2c), (2d), and (2e) are imposed to (8b), (8c), and (11), and the orthogonality of the spherical harmonics on the unit sphere is used.

Initially, condition (2b) is analyzed. Using Eqs. 39a and 39b in Eq. 2b, one obtains

$$\left(\frac{a-t}{a}\right)^l b_n + \left(\frac{a}{a-t}\right)^{l+1} c_n = \left(\frac{a-t}{a}\right)^l d_n \tag{14}$$

Using Eqs. 42a and 42b in Eq. 2d, it can be found that

$$\tilde{k}_s \left(l \frac{(a-t)^{l-1}}{a^l} b_n - (l+1) \frac{a^{l+1}}{(a-t)^{l+2}} c_n + \sqrt{\frac{4\pi}{3}} \delta_{n,e01} \right) = \tilde{k}_c \left(l \frac{(a-t)^{l-1}}{a^l} d_n + \sqrt{\frac{4\pi}{3}} \delta_{n,e01} \right) \tag{15}$$

Now, the continuity condition (2c) is applied. From Eq. 2c, it can be found that

$$b_n + c_n = a_n + \sum_{n' \in I} S_{n'n} a_{n'} - f_a a_{e01} \delta_{n,e01} \tag{16}$$

Finally, the interface condition (2e) is applied to obtain

$$\tilde{k}_s \left(\frac{l}{a} b_n - \frac{l+1}{a} c_n + \sqrt{\frac{4\pi}{3}} \delta_{n,e01} \right) = -\frac{l+1}{a} a_n + \frac{l}{a} \sum_{n' \in I} S_{n'n} a_{n'} - \frac{f_a}{a} a_{e01} \delta_{n,e01} + \sqrt{\frac{4\pi}{3}} \delta_{n,e01} \tag{17}$$

Solving for d_n in (14) provides

$$d_n = b_n + \left(\frac{a}{a-t}\right)^{2l+1} \tag{18}$$

Substituting (18) into (15) and solving for c_n , it can be found that

$$c_n = m(l)b_n + a \sqrt{\frac{4\pi}{3}} m(1) \delta_{n,e01} \tag{19}$$

where

$$m(l) = \frac{l(1 - \tilde{k}_c/\tilde{k}_s)}{l+1 + \tilde{k}_c/\tilde{k}_s} \left(\frac{a-t}{a}\right)^{2l+1} \tag{20}$$

Substituting (19) into (16) and solving for b_n results in

$$b_n = \frac{1}{1+m(l)} \left(a_n + \sum_{n' \in I} S_{n'n} a_{n'} - f_a a_{e01} \delta_{n,e01} + a \sqrt{\frac{4\pi}{3}} m(1) \delta_{n,e01} \right) \tag{21}$$

Substituting (19) into (17) results in

$$\tilde{k}_s(l - (l+1)m(l))b_n + (l+1)a_n - l \sum_{n' \in I} S_{n'n} a_{n'} + f_a a_{e01} \delta_{n,e01} = a \sqrt{\frac{4\pi}{3}} (1 - \tilde{k}_s + 2\tilde{k}_s m(1)) \delta_{n,e01} \tag{22}$$

By substituting (21) into (22), an infinite set of equations is determined for the coefficients a_n

$$\sum_{n' \in I} M_{n'n} a_{n'} = g \delta_{n,e01} \tag{23}$$

where the infinite coefficient matrix $M_{n'n}$ and the load g are defined by

$$M_{n'n} = \left(\tilde{k}_s \frac{l - (l+1)m(l)}{1+m(l)} (1 - f_a \delta_{n,e01}) + l + 1 + f_a \delta_{n,e01} \right) \delta_{n'n} + \left(\tilde{k}_s \frac{l - (l+1)m(l)}{1+m(l)} - l \right) S_{n'n} \tag{24}$$

and

$$g = a \sqrt{\frac{4\pi}{3}} (1 - \tilde{k}_s + 2\tilde{k}_s m(1)) + a \sqrt{\frac{4\pi}{3}} m(1) \tilde{k}_s \frac{1 - 2m(1)}{1+m(1)} \tag{25}$$

It is noted that for solid spheres, that is, $t = 0$, the system of equations (23) coincides with the governing equations in [32].

By solving Eq. 23 for a_n and by substituting into (21) and (19), we find the coefficients b_{e01} and c_{e01} whose values determine the effective relative conductivity of the particulate composite as stated in Eq. 13.

Asymptotic solution

A closed form expression for the effective conductivity for small a , therefore moderately small volume fractions, is now developed. As shown in [32], the quantity $S_{n'n}$ defining the infinite matrix in (24) satisfies

$$S_{n'n} = O(a^{l+l+1}) \tag{26}$$

In addition, due to the lattice symmetry $S_{e01e01} = S_{e01e23} = S_{e23e01} = 0$. Therefore, the lowest order contribution is provided only by the two terms S_{e03e01} and S_{e01e03} that contribute as $O(a^5)$. As a consequence, neglecting terms of the order $O(a^7)$ the system (23) can be written as

$$\mu_{11}a_{e01} + \mu_{31}S_{e03e01}a_{e03} = g \tag{27a}$$

$$\mu_{13}S_{e01e03}a_{e01} + \mu_{33}a_{e03} = 0 \tag{27b}$$

The product $S_{e03e01}S_{e01e03}$ has been evaluated numerically in [32] and equals approximately $155a^{10}$. Therefore, by replacing the above values for b_{e01} and c_{e01} in Eq. 13 we find the effective relative thermal conductivity of the hollow particle filled composite. The truncation error is of the order of a^{15} .

For the case of relatively low volume fractions of microballoons, the contribution due to $S_{e03e01}S_{e01e03}$ can be discarded obtaining an estimate whose truncation error is of the order of a^{10} . In this case, the expression of the effective conductivity simplifies to

$$\tilde{k}^h = 1 - \frac{3f_a \left((1 - \tilde{k}_s)(\tilde{k}_c + 2\tilde{k}_s) + (\tilde{k}_s - \tilde{k}_c)(1 + 2\tilde{k}_s) \frac{f_a - t}{f_a} \right)}{(\tilde{k}_c + 2\tilde{k}_s)(2 + \tilde{k}_s - f_a(\tilde{k}_s - 1)) + (\tilde{k}_s - \tilde{k}_c)(2 - 2\tilde{k}_s + f_a(1 + 2\tilde{k}_s)) \frac{f_a - t}{f_a}} \tag{32}$$

where

$$\mu_{11} = \tilde{k}_s(1 - f_a) \frac{1 - 2m(1)}{1 + m(1)} + 2 + f_a \tag{28a}$$

$$\mu_{31} = \tilde{k}_s \frac{1 - 2m(1)}{1 + m(1)} - 1 \tag{28b}$$

$$\mu_{13} = \tilde{k}_s \frac{3 - 4m(3)}{1 + m(3)} - 3 \tag{28c}$$

$$\mu_{33} = \tilde{k}_s \frac{3 - 4m(3)}{1 + m(3)} + 4 \tag{28d}$$

The approximate solution of the linear system described by Eqs. 27a and 27b is

$$a_{e01} \simeq \left(\frac{1}{\mu_{11}} + \frac{\mu_{31}\mu_{13}}{\mu_{11}^2\mu_{33}} S_{e03e01}S_{e01e03} \right) g \tag{29a}$$

$$a_{e03} \simeq - \frac{\mu_{13}}{\mu_{11}\mu_{33}} S_{e01e03} g \tag{29b}$$

Consequently from Eqs. 19 and 21, the coefficients b_{e01} and c_{e01} are

$$b_{e01} \simeq \frac{1}{1 + m(1)} \left(\frac{g(1 - f_a)}{\mu_{11}} - a\sqrt{\frac{4\pi}{3}}m(1) \right) + \frac{1}{1 + m(1)} \left(g \frac{\mu_{13}}{\mu_{11}^2\mu_{33}} (\mu_{31}(1 - f_a) - \mu_{11}) S_{e03e01}S_{e01e03} \right) \tag{30}$$

and

$$c_{e01} \simeq \frac{m(1)}{1 + m(1)} \left(\frac{g(1 - f_a)}{\mu_{11}} + a\sqrt{\frac{4\pi}{3}} \right) + \frac{m(1)}{1 + m(1)} g \left(\frac{\mu_{13}}{\mu_{11}^2\mu_{33}} (\mu_{31}(1 - f_a) - \mu_{11}) S_{e03e01}S_{e01e03} \right) \tag{31}$$

For two-phase composites, that is when $t = 0$, Eq. 32 coincides with the well-known Maxwell–Garnett formula, see for example [28]. For thin shells, a further approximation may be performed to obtain a manageable and meaningful expression by linearizing the approximate effective relative conductivity in Eq. 32 for small wall thicknesses t . In this case, the effective relative conductivity Eq. 13 becomes

$$\tilde{k}^h = 1 - \frac{3f_a(1 - \tilde{k}_c)}{2 + \tilde{k}_c - f_a(\tilde{k}_c - 1)} + \frac{9f_a(2\tilde{k}_s^2 - \tilde{k}_c\tilde{k}_s - \tilde{k}_c^2)}{\tilde{k}_s(2 + f_a + \tilde{k}_c(1 - f_a))^2} \frac{t}{a} \tag{33}$$

The first two summands in Eq. 33 correspond to the effective relative conductivity of a two-phase composite with solid inclusions of radius a and relative conductivity \tilde{k}_c computed with the Maxwell–Garnett formula. The last summand in Eq. 33 corrects the Maxwell–Garnett formula to account for the presence of the thin shells.

Finite element analysis

Problem formulation

For the FEA of the unit cell problem described in Problem statement section, it is convenient to transform the original formulation in Eq. 1 into a simpler formulation, where periodicity conditions and interface conditions are removed.

Note that, due to the symmetry of the problem, the periodicity condition (2f) can be replaced by the mixed boundary conditions

$$\frac{\partial \psi}{\partial y_1}(\pm 1/2e_1) = 0 \quad (34a)$$

$$\frac{\partial \psi}{\partial y_2}(\pm 1/2e_2) = 0 \quad (34b)$$

$$\psi(\pm 1/2e_3) = 0 \quad (34c)$$

In addition, due to the linearity of the problem, we can express the solution $\psi(y)$ as the summation of a particular solution $\psi^p(y)$ of the Laplace equation in the unit cell, satisfying conditions (2b), (2c), (2d), and (2e) and a function $\Psi(y)$ solving the following mixed boundary value problem

$$\Delta \Psi(y) = 0 \quad y \in Y \setminus (\partial \Omega_{a-t} \cup \partial \Omega_{a-t}) \quad (35a)$$

$$\Psi(y^+) = \Psi(y^-) \quad y \in \partial \Omega_a \quad (35b)$$

$$\Psi(y^+) = \Psi(y^-) \quad y \in \partial \Omega_{a-t} \quad (35c)$$

$$\tilde{k}_s v \cdot \nabla \Psi(y^+) = \tilde{k}_c v \cdot \nabla \Psi(y^-) \quad y \in \partial \Omega_{a-t} \quad (35d)$$

$$v \cdot \nabla \Psi(y^+) = \tilde{k}_s v \cdot \nabla \Psi(y^-) \quad y \in \partial \Omega_a \quad (35e)$$

$$\frac{\partial \Psi}{\partial y_1}(\pm 1/2e_1) = -\frac{\partial \psi^p}{\partial y_1}(\pm 1/2e_1) \quad (35f)$$

$$\frac{\partial \Psi}{\partial y_2}(\pm 1/2e_2) = -\frac{\partial \psi^p}{\partial y_2}(\pm 1/2e_2) \quad (35g)$$

$$\Psi(\pm 1/2e_3) = -\psi^p(\pm 1/2e_3) \quad (35h)$$

A particular solution of the problem is

$$\psi^p(y) = -a \sqrt{\frac{4\pi}{3}} v_{e_01}(y) \equiv -y_3 \quad (36)$$

Therefore, from Eqs. 35f, 35g, and 35h the mixed boundary conditions required to determine Ψ are

$$\frac{\partial \Psi}{\partial y_1}(\pm 1/2e_1) = 0 \quad (37a)$$

$$\frac{\partial \Psi}{\partial y_2}(\pm 1/2e_2) = 0 \quad (37b)$$

$$\Psi(\pm 1/2e_3) = \pm 1/2 \quad (37c)$$

These boundary conditions correspond to leaving four surfaces of the unit cell free and to imposing a constant temperature on the remaining two surfaces. Specifically, constant temperatures of equal value and opposite sign are imposed on the two surfaces orthogonal to e_3 that induce a thermal gradient in the unit cell.

Once the solution field Ψ is determined using the FEA, the effective thermal conductivity is found by replacing $\psi = \psi^p + \Psi$ into Eq. 6, yielding

$$\begin{aligned} \tilde{k}^h = 1 + (\tilde{k}_s - 1) \int_{\partial \Omega_a} \Psi(y) v(y) \cdot e_3 \, dA \\ + (\tilde{k}_c - \tilde{k}_s) \int_{\partial \Omega_{a-t}} \Psi(y) v(y) \cdot e_3 \, dA \end{aligned} \quad (38)$$

The set of equations (35) with boundary conditions (37) can be solved using any commercial finite element code, and the effective relative conductivity can be estimated using Eq. 38.

Computer implementation

The finite element solution of the set of equations (35) with boundary conditions (37) is performed using Ansys 11.0. The analysis is conducted on the three-dimensional unit cell displayed in Fig. 2. The unit cell consists of a spherical core (air) surrounded by a concentric spherical shell (microballoon) embedded in a unit cube of the matrix material.

Symmetry conditions are used to simplify the FEA to only one quarter of the unit cell. The finite element model of the unit cell is shown in Fig. 3. The center of the shell and core as well as the cube are set at the origin of the

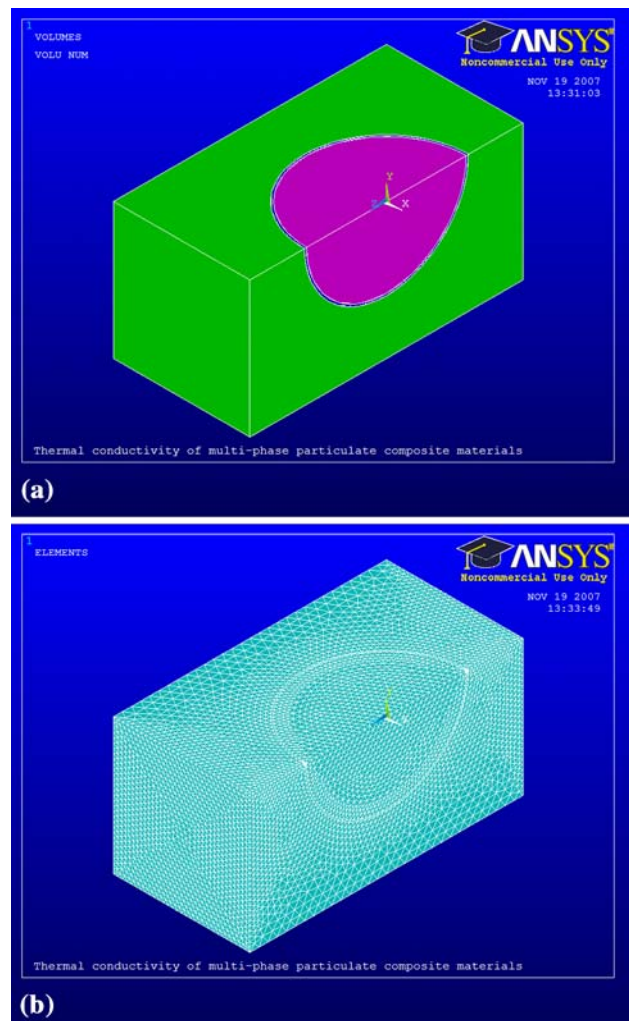


Fig. 3 **a** The three-phase composite microstructure and **b** the meshed model used for FEA

coordinate system. In the unit cell problem, the outer radius of the microballoon, a , is varied between 0 and 0.499. The limiting case is taken as 0.499 because at 0.5 the radius of the microballoon becomes equal to the half-length of the unit cell and the matrix becomes discontinuous. The matrix resin is assumed to be vinyl ester and microballoons are assumed to be made of borosilicate glass. The thermal conductivities of the matrix polymer, microballoons, and air are assumed to be 0.25, 1.1, and 0.01 W/mK, respectively. For these parameters, the relative thermal conductivities of the shell and core materials are $\tilde{k}_s = 4.4$ and $\tilde{k}_c = 0.04$, respectively.

To satisfy the continuity conditions (35b) and (35c), the contacts between the matrix and the shell and the shell and the core are defined as “glued.” Thermal element used in the analysis is “Solid87-10 node tetrahedral thermal solid,” that is well suited for meshing curved geometries. Solid87 has one degree of freedom, which is temperature, at each node. Boundary conditions are constant temperature on the two opposite surfaces of the finite element model orthogonal the unit vector e_3 in Fig. 2. On the remaining four sides, orthogonal to the unit vectors e_1 and e_2 , heat flux is set at zero. The solution is run in a single step. The total number of elements in the finite element model is between 128,669 and 395,030 depending upon the shell thickness and volume fractions. A larger number of elements were

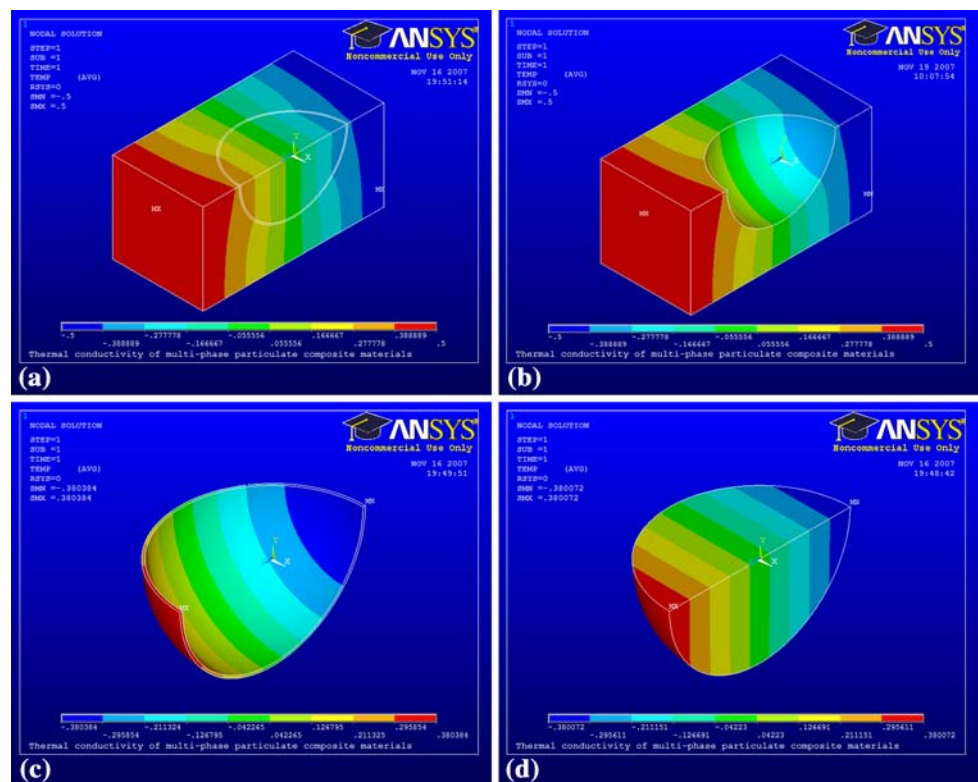
used in geometries comprising thinner shells. The number of elements was chosen to guarantee a fully converged solution.

Finite element analysis results provides only the temperature distribution within the unit cell. Therefore, a Matlab routine was developed to postprocess the data and to compute the relative effective conductivity from mesh and nodal temperatures. The FEA results provide the temperature distribution in the model. In order to extract the relative effective conductivity through the FEA according to Eq. 38, numerical integration over the inner and outer surfaces of the shell are required. Nodes on the inner and outer surfaces of the shell along with the corresponding elements are identified from the mesh file of ANSYS. The associated nodal temperatures are identified from the results file.

Discussion

The FEA results for the nodal temperatures are shown in Fig. 4a for a particulate composite with particles of relative wall thickness $t/a = 0.025$ and relative outer radius $a = 0.3$. It can be observed that the temperature in the matrix increases significantly in the vicinity of the inclusion, and remains almost unaltered inside the core. The

Fig. 4 The variation in the temperature within the **a** composite, **b** matrix, **c** microballoon shell, and **d** air core. The figures represent one quarter of the geometry



variation in the temperature within the matrix, the shell, and the core are displayed in Fig. 4b, c, and d, respectively. The temperature values obtained from the FEA are used in estimating the relative thermal conductivity of the composite as explained in the section above.

The thermal conductivity values calculated for composites containing thin hollow particles of relative thickness $t/a = 0.025$ and $t/a = 0.05$ in the entire range of $0 < a < 0.5$ using the proposed model are compared with the Hashin–Shtrikman bounds in equation (7) in Fig. 5a and b, respectively. Reported modeling results refer to the closed-form solution (32), that is truncated at the a^{10} , and to its approximation for thin shells in Eq. 33.

As illustrated through Fig. 5, the theoretical values are within the bounds. The approximate solution in Eq. 33 is superimposed to the closed-form solution in Eq. 32 for

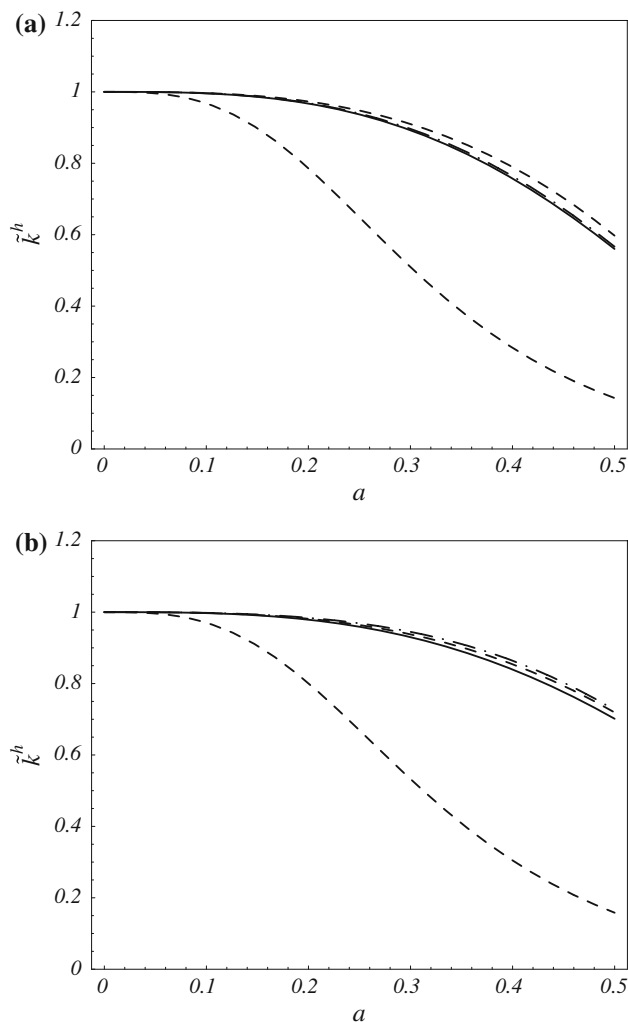


Fig. 5 Comparison between relative thermal conductivity computed using Eqs. 32 (solid line) and 33 (dotted-dashed line) and Hashin–Shtrikman bounds (dashed lines) for **a** $t/a = 0.025$ and **b** $t/a = 0.05$

very thin shells, that is, for $t/a < 0.025$. The approximate solution shows instead a small departure from the closed-form solution in Eq. 32 for moderately thin shells, that is, for $0.025 < t/a < 0.05$, only for $a > 0.4$. The dimensionless parameter a serves as a means to determine the volume fraction of microballoons in the composite material. For example, at the values of $a = 0.1, 0.3$ and 0.499 the volume fraction of microballoons in the composite is 0.42%, 11.31%, and 52.05%, respectively. Hence, the approximate solution can be used to obtain accurate estimates of thermal conductivity of composites containing <30% by volume of moderately thin-walled microballoons with $t/a < 0.05$. The computed values of relative thermal conductivity remains within the Hashin–Shtrikman bounds for the entire range of shell thickness.

As illustrated in Fig. 5, the closed-form solution (32) is relatively close to the upper bound, while it is well separated from the lower bound. This is due to the relevant difference between the thermal conductivities of the materials comprising the unit cell, specifically to the low relative thermal conductivity of the core material.

Once the validity of the solutions against the Hashin–Shtrikman bounds is confirmed, the general trends in the relative thermal conductivity values are observed. The thermal conductivity values for various microballoons' wall thickness computed using Eq. 32 are compared with FEA results in Fig. 6a. It can be observed that the results obtained from both methods agree with each other, validating the theoretical results. Figure 6b compares the FEA results to the forecasts of the approximate solution in Eq. 33. In accordance with Fig. 5, the thin shell approximation provides good predictions for shells of relative thickness <5%. As the wall thickness increases, the approximate solution becomes less unreliable. However, in practical conditions, thin shells are generally preferred in synthesizing hollow particle filled composites to limit the structural density. The approximate solution in Eq. 33 can be useful in developing differential models well suited to study random dispersion of thin-walled hollow particles in a wide volume fraction range [29, 30].

The overall thermal characteristics of the particulate composite can be tailored through the selection of constituent materials, volume fractions of inclusions and thickness of microballoons. In the considered sample case, the thermal conductivity of the microballoon is 4.4 times higher than the matrix material, hence, microballoon becomes an effective channel of heat transfer within the unit cell. In such a case, the wall thickness of microballoon plays an important role in determining the overall thermal conductivity of the specimen. However, depending on the design requirements of the application, thermal properties of hollow particle filled composites can be optimally tailored.

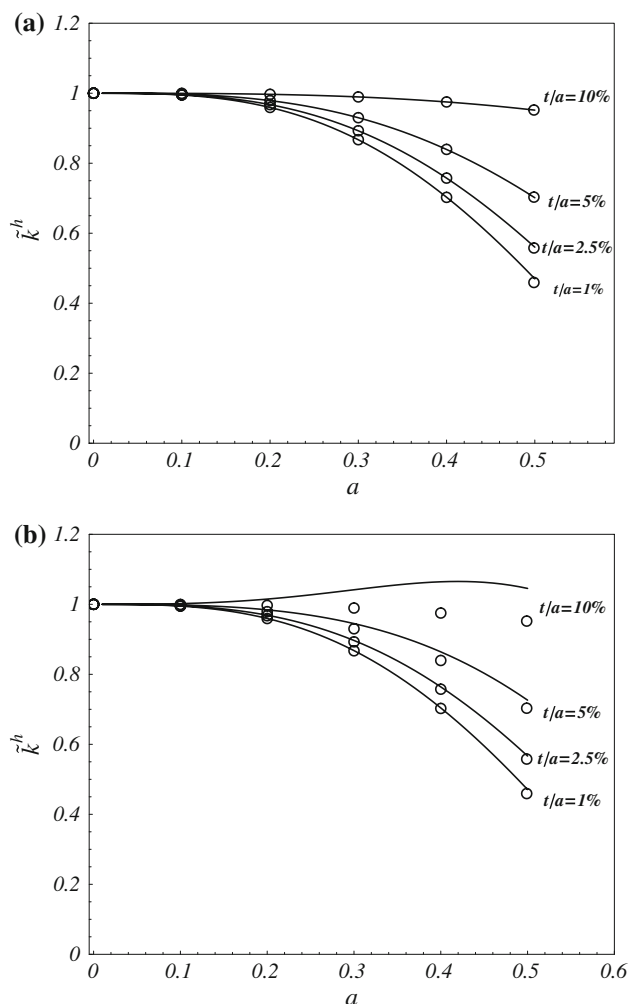


Fig. 6 Validation of theoretically calculated values of thermal conductivity of syntactic foams with finite element analysis results **a** Eq. 32 and **b** Eq. 33. Solid lines are the theoretical values and circles are the FEA results

Conclusions

An analytical model to predict the thermal conductivity of particulate composites is developed in this study using homogenization techniques. The model, which builds on the framework proposed in [32] for solid particle filled composites, is applicable to composites containing solid or hollow spherical particles in a matrix material. The model is validated with FEA results for vinyl ester matrix syntactic foams containing glass microballoons. It is observed that the thermal conductivity values predicted by the model match closely with the FEA results. A simplified approximation of the model suitable for practical design is also presented. The approximate solution is successful in predicting the thermal conductivity of composites containing thin-walled microballoons in volume up to 30%. The results show that the thermal conductivity of syntactic foams is highly sensitive to the microballoon wall thickness.

The predictive capabilities are expected to result in better tailoring of syntactic foams, and particulate composites in general, for a diverse set of applications including space structures.

Acknowledgements This work is supported by the Office of Naval Research grant N00014-07-1-0419 with Dr. Y.D.S. Rajapakse as the Program Manager and by the National Science Foundation Grant CBET-0619193.

Appendix A: solutions to the Laplace equation

The functions u_n and v_n are defined in terms of the spherical harmonics as

$$u_n(y) = \left(\frac{a}{\rho}\right)^{l+1} Y_n(\theta, \phi) \tag{39a}$$

$$v_n(y) = \left(\frac{\rho}{a}\right)^l Y_n(\theta, \phi) \tag{39b}$$

The spherical harmonics are defined by

$$Y_{eml}(\theta, \phi) = \sqrt{\frac{2 - \delta_{m,0}}{2\pi}} \sqrt{\frac{2l + 1}{2} \frac{(l - m)!}{(l + m)!}} P_l^m(\cos \theta) \cos(m\phi) \tag{40a}$$

$$Y_{oml}(\theta, \phi) = \sqrt{\frac{2 - \delta_{m,0}}{2\pi}} \sqrt{\frac{2l + 1}{2} \frac{(l - m)!}{(l + m)!}} P_l^m(\cos \theta) \sin(m\phi) \tag{40b}$$

where P_l^m denotes the Associated Legendre functions. The spherical harmonics are orthonormal on the unit sphere, that is

$$\int_0^{2\pi} \int_0^\pi Y_{\sigma ml} Y_{\sigma' m' l'} \sin \theta \, d\theta \, d\phi = \delta_{\sigma, \sigma'} \delta_{l, l'} \delta_{m, m'} \tag{41}$$

We note that (40a) is an even function of ϕ while (40b) is an odd function of ϕ . We also note if l is an odd integer and m is an even integer then (40a) is an odd function of $\cos \theta$.

The partial derivatives of the basis functions u_n and v_n with respect to the radial coordinate ρ are

$$\frac{\partial u_n(y)}{\partial \rho} = -\frac{l + 1}{a} \left(\frac{a}{\rho}\right)^{l+2} Y_n(\theta, \phi) \tag{42a}$$

$$\frac{\partial v_n(y)}{\partial \rho} = \frac{l}{a} \left(\frac{\rho}{a}\right)^{(l-1)} Y_n(\theta, \phi) \tag{42b}$$

References

1. Narkis M, Kenig S, Puterman M (1984) Polym Compos 5:159
2. Shutov FA (1991) Syntactic polymeric foams. Hanser Publishers, New York

3. Bibin J, Nair CPR, Devi KA, Ninan KN (2007) *J Mater Sci* 42:5398. doi:[10.1007/s10853-006-0778-0](https://doi.org/10.1007/s10853-006-0778-0)
4. Koopman M, Chawla KK, Carlisle KB, Gladysz GM (2006) *J Mater Sci* 41:4009
5. Bunn P, Mottram JT (1993) *Composites* 24:565
6. Kishore, Shankar R, Sankaran S (2005) *Mater Sci Eng A* 412:153
7. Rohatgi P, Kim J, Gupta N, Alaraj S, Daoud A (2006) *Compos Part A Appl Sci Manuf* 37:430
8. Balch DK, Dunand DC (2006) *Acta Mater* 54:1501–1511
9. Gupta N, Woldeesenbet E, Kishore (2002) *J Mater Sci* 37:3199. doi:[10.1023/A:1016166529841](https://doi.org/10.1023/A:1016166529841)
10. Gupta N, Woldeesenbet E, Mensah P (2004) *Compos A Appl Sci Manuf* 35:103
11. Gupta N, Nagorny R (2006) *J Appl Polym Sci* 102:1254
12. Bardella L, Genna F (2001) *Int J Solids Struct* 38:7235
13. Huang JS, Gibson LJ (1993) *J Mech Phys Solids* 41:55
14. Porfiri M, Gupta N (2008) *Compos B*. doi:[10.1016/j.compositesb.2008.09.002](https://doi.org/10.1016/j.compositesb.2008.09.002)
15. Tagliavia G, Porfiri M, Gupta N (2008) *J Compos Mater*, Accepted, in print
16. Karthikeyan CS, Sankaran S, Kishore (2007) *Polym Adv Technol* 18:254
17. Kishore, Shankar R, Sankaran S (2005) *J Appl Polym Sci* 98:680
18. Shabde V, Hoo K, Gladysz G (2006) *J Mater Sci* 41:4061. doi:[10.1007/s10853-006-7637-x](https://doi.org/10.1007/s10853-006-7637-x)
19. Rohatgi PK, Gupta N, Alaraj S (2006) *J Compos Mater* 40:1163
20. Rayleigh L (1892) *Philos Mag* 34:481
21. McPhedran RC, McKenzie DR (1978) *Proc R Soc Lond A* 359:45
22. McKenzie DR, McPhedran RC, Derrick GH (1978) *Proc R Soc Lond A* 362:211
23. Cheng H, Torquato S (1997) *Proc R Soc Lond A* 453:145
24. Nicorovici NA, McPhedran RC, Milton GW (1994) *Proc R Soc Lond A* 442:599
25. Moosavi A, Sarkomaa P, Polashenski W (2003) *Appl Phys A Mater Sci Process* 77:441
26. Awrejcewicz J, Andrianov IV, Manevitch LI (1998) *Asymptotic approaches in nonlinear dynamics*. Springer, Berlin
27. Cioranescu D, Saint Jean Paulin J (1999) *Homogenization of reticulated structures*. Springer, Berlin
28. Torquato S (2001) *Random heterogeneous materials: microstructure and macroscopic properties*. Springer, Berlin
29. Pal R (2005) *Mater Sci Eng A* 412:71
30. Pal R (2005) *Compos B Eng* 36:513
31. Carson JK, Lovatt SJ, Tanner DJ, Cleland AC (2005) *Int J Heat Mass Trans* 48:2150
32. Kristensson G (2003) *Progr Electromagnet Res* 42:1
33. Fiedler T, Solrzano E, Ochsner A (2008) *Mater Lett* 62:1204
34. Liang J, Li FH (2007) *Polym Test* 26:419
35. Song YS, Youn JR (2006) *Carbon* 44:710
36. Rankin RA (1963) *An introduction to mathematical analysis*. Pergamon Press, New York